Int. J. Nanosci. Nanotechnol., Vol. 10, No. 1, Mar. 2014, pp. 45-54

Synthesis and Characterization of $La_{0.6}Sr_{0.4}NiO_3$ Nanocrystals via a Simple Co-precipitation Method in the Present of Surfactant

M. Khorasani-Motlagh*, H. Vahidi, M. Noroozifar

Department of Chemistry, University of Sistan & Baluchestan, Zahedan, I. R. Iran

(*) Corresponding author: mkhorasani@chem.usb.ac.ir
(Received:23 May 2013 and Accepted: 12 Jan. 2014)

Abstract:
The perovskite-type oxides strontium-substituted lanthanum nickelate (LSNO) were prepared by a coprecipitation method in the present of octanoic acid as surfactant. The phase composition, morphology, lattice parameters and size of nanoparticles in these materials were characterized through Fourier transform infrared spectroscopy (FT-IR), X-ray diffraction (XRD), scanning electron microscopy (SEM) and energy dispersive X-ray (EDX) on the resultant powders at room temperature. This method produced oxides with nanoparticles following the orthorhombically distorted crystal structure. The LSNO were synthesized in homogeneous nanosize particles of about 53 nm.
Keywords: *Perovskite-type, Nanoparticles, Co-precipitation, Surfactant, XRD, SEM, EDX*

1. INTRODUCTION

Mixed oxides with perovskite and perovskite-like structures are preferred objects of investigation in the search for materials with high oxygen ionic transfer [1,2]. Perovskite like mixed oxides, with general formula ABO_3, showed suitable catalysts for oxidation of light hydrocarbons particularly methane [3,4].

Perovskite-like oxides can be tailored to create a wide family of catalysts, by varying either the A-site or the B-site metal ion, or both. Indeed, the catalytic activity of a perovskite can be modified by inserting proper transition metal ions. Moreover, partial substitution at A-site with another A' metal cation to give $A_{1-x}A'_xBO_3$ can strongly affect catalytic activity, due to stabilization of unusual oxidation states of the B component and to simultaneous formation of structural defects created by such a substitution. The perovskite-type oxides are versatile for many catalytic reactions including those of the partial and complete oxidation of hydrocarbons [5,6].

The perovskite oxides can stand substantial isomorphic substitution at the cationic sites, and it is possible to generate cationic and anionic vacancies and to regulate the redox ability of B-site ions by tuning the elemental composition of the material [7]. The perovskite oxides $A_{1-x}A'_xBO_{3-\delta}$ (A = La, A′= Ca, Sr, B = Co, Fe, Ni, etc.) have been used as a sensing material in oxygen [8], carbon monoxide, hydrocarbon [9], and nitrite oxide [10,11] sensors. The sensing principle of these sensors is mainly related to the catalytic oxidation of the compounds to be analyzed in the presence of the oxygen vacancies. Since Co^{+z}, Fe^{+z} and Ni^{+z} cations have different oxidation states, the charge neutrality can be maintained by forming the oxygen vacancies and changing in the valence state of the cations.

Therefore, these structures have an oxygen deficiency, δ, due to the high oxygen vacancy concentration and can show a good electrical

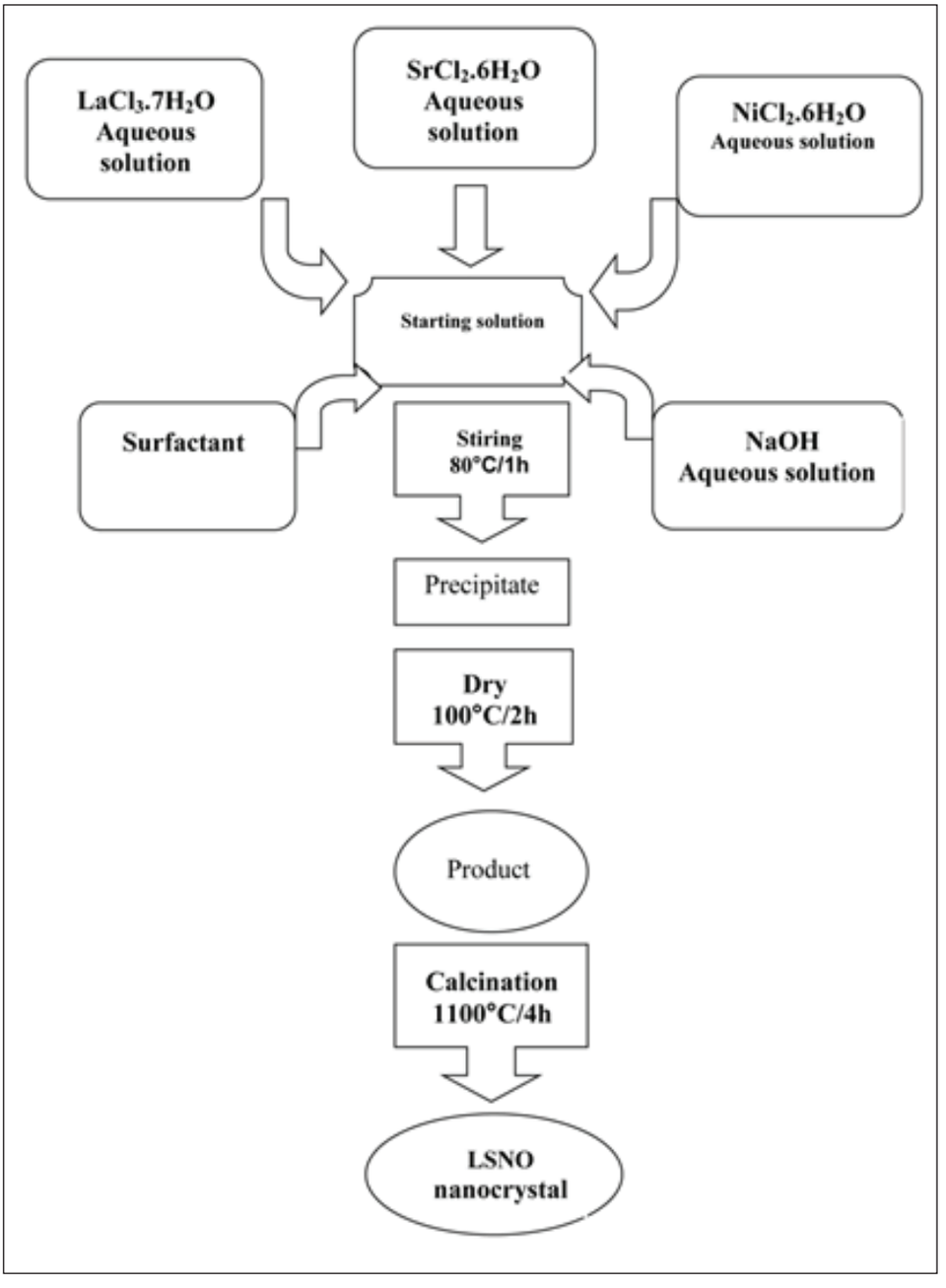

Figure 1: *Diagram of the chemical process for the formation of $La_{0.6}Sr_{0.4}NiO_3$ nanocrystals.*

conductivity, catalytic, mechanical, and colossal magnetoresistance (CMR) properties which have attracted a lot of attention. [12–16]

In this work, we prepared perovskite-type $La_{0.6}Sr_{0.4}NiO_3$ (LSNO) nanocrystals by a coprecipitation method in aqueous solution. The crystalline phase with perovskite structure can be obtained by calcining the precursor at 1100°C. The characterizations of the nanocrystalline perovskite were demonstrated by FT-IR, XRD, SEM and EDX.

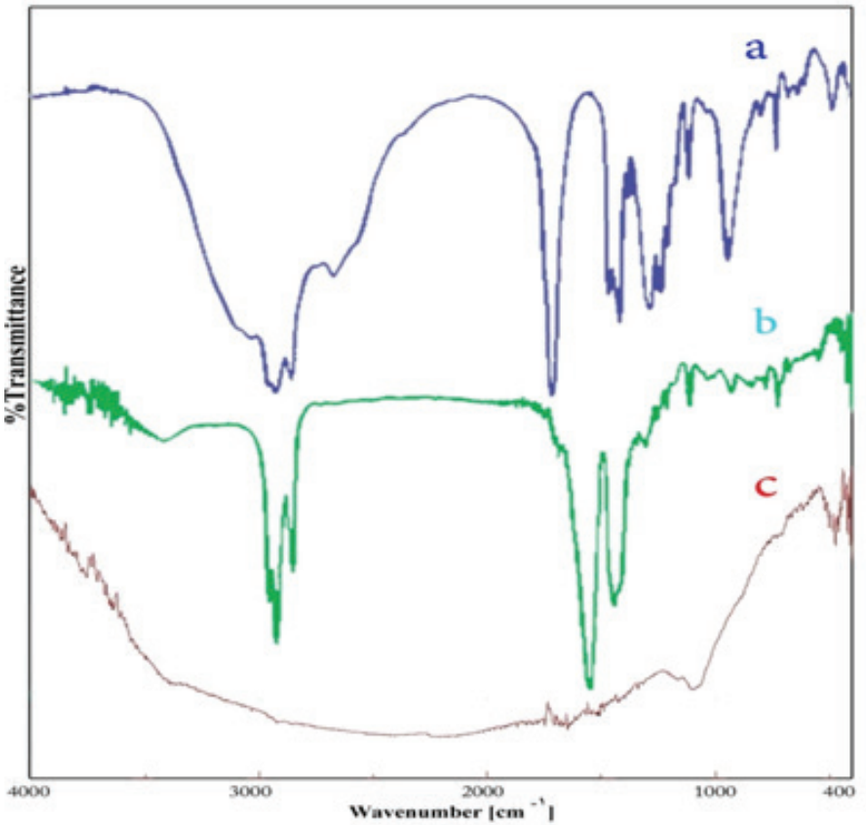

Figure 2: *FT-IR spectra of (a) octanoic acid, (b) sample before furnace, (c) sample after furnace.*

2. EXPERIMENTAL

2.1. Materials

All materials were purchased from Merck Co. All solutions were prepared using double distilled water.

2.2. Characterization

The FT-IR spectra of the final product were recorded in a JASCO–460 plus FT-IR spectrophotometer in the range from 400 to 4000 cm^{-1} in KBr pellets. X-ray powder diffraction (XRD) analysis was conducted on a Philips analytical PC-APD X-ray diffractometer with graphite monochromatic Cu Kα radiation to verify the formation of products. SEM measurements were carried out using a Philips XL30 Scanning electron microscope equipped with an energy dispersive X-ray (EDX) spectroscopy.

2.3. Synthesis of $La_{0.6}Sr_{0.4}NiO_3$ (LSNO) nano-crystals

Perovskite oxides with molecular composition $La_{0.6}Sr_{0.4}NiO_3$ were synthesized by co-precipitation precursor method. In this method, first, $LaCl_3.7H_2O$ (0.06M), $SrCl_2 \bullet 6H_2O$ (0.04M) and $NiCl_2 \bullet 6H_2O$ (0.1M), were dissolved as per stoichiometry in 30 ml distilled water. A specified amount of octanoic acid was added to the solution as a surfactant and coating material. A 1.5 M solution of sodium hydroxide was prepared and slowly added to the salt solution drop wise. The pH of the solution was constantly monitored as the sodium hydroxide solution was added.

The reactants were constantly stirred using a magnetic stirrer until a pH level of 6–7 was reached. The resulting solution was allowed to evaporate slowly at 80°C until a viscous gel was obtained

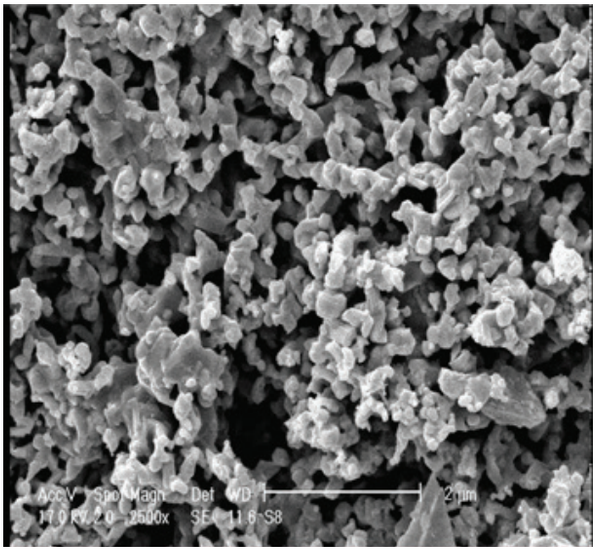

Figure 3: *Scanning electron micrograph of* $La_{0.6}Sr_{0.4}NiO_3$ *powder.*

and the precipitation was completed. The obtained products were dried at 100˚C for 2 h and calcined at 1100°C in air for 4 h (Figure 1). The final samples were then confirmed by different techniques, such as XRD‹ FT-IR‹ SEM‹ EDX, etc.

3. RESULTS AND DISCUSSION

Fourier transform infrared spectra of octanoic acid (a), perovskite LSNO before furnace (b), and perovskite LSNO after furnace (c), in the frequency range from 4000 to 400 cm^{-1}, are shown in Figure 2. The spectrum of the LSNO before furnace showed absorption band around 2600-3000 cm^{-1} attributed to acid's OH that disappeared in spectrum after furnace. Also, the broad band in the range of 3300-3500 cm^{-1} attributed to ν (OH) of the lattice water molecules was seen. In the FT-IR spectrum of the final product, there was a weak absorptive band at about 560 cm^{-1} which correspond to M–O (M=Ni, Sr, La) stretching vibration of perovskite LSNo. Scanning electron micrographs of $La_{0.6}Sr_{0.4}NiO_3$ powders is shown in Figure 3. Morphology of all nano powders seemed to be almost similar and fine spherical features. For further demonstration, EDX was performed on LSNO nanocrystals. The EDX spectrum given in Figure 4 shows the presence of strontium, lanthanum and nickel as the elementary components. The atomic percentage of three elements strontium, lanthanum and nickel is shown in Figure 4.

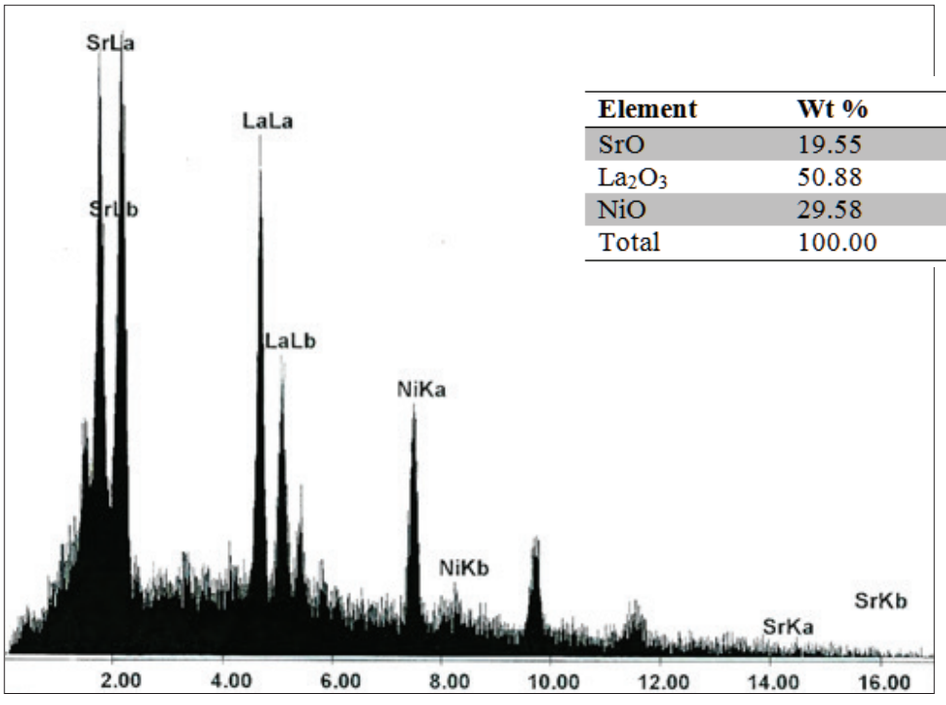

Element	Wt %	At %
SrO	19.55	25.47
La_2O_3	50.88	21.08
NiO	29.58	53.45
Total	100.00	100.00

Figure 4: *EDX analysis of* $La_{0.6}Sr_{0.4}NiO_3$ *nano-sized powders.*

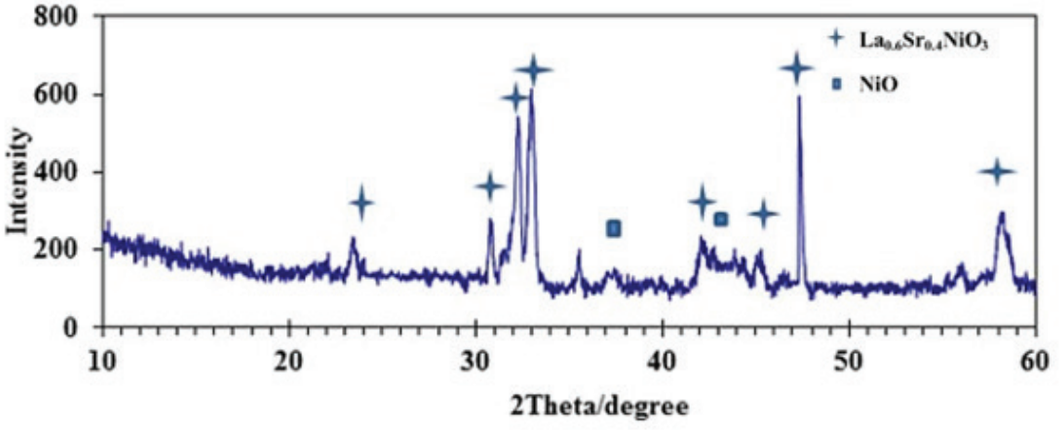

Figure 5: *XRD pattern of $La_{0.6}Sr_{0.4}NiO_3$ nanocrystals.*

The XRD powder pattern of strontium-substituted lanthanum nickelate (LSNO) calcined at 1100°C [8] is given in Figure 5. This Figure clearly indicates the formation of the crystalline orthorhombic perovskite phase (JCPDS pattern 34-1028). A careful perusal of Figure 5 shows, further, that the XRD spectra for the LSNO have, in fact, additional weak diffraction lines, of which correspond to NiO. From the XRD data and Debye–Scherrer equation [17], the crystallite size of LSNO nanoparticles was calculated 53 nm.

The epitaxial growth of crystallites, the slow nucleation, and the growth rates result in the formation of nanoparticles. On the contrary, if NaOH solution is quickly added into the mixture solution, the solute is consumed rapidly and the epitaxial growth of crystallites is effectively inhibited. Meanwhile, the quick addition of NaOH solution can provide a quick rate to the crystal growth. The faster growth rate results in the crystal growth being considerably less selective in directions and hence spherical LSNO nanoparticles are produced.

The shape and size of LSNO nanoparticles can be further tuned by adding small amounts of surfactants. The result demonstrates that the presence of small amounts of octanoic acid leads to the shape change of LSNO products. The use of a surfactant to control the morphological evolution of nanoparticles has been extensively explored. It is generally accepted that the surfactant kinetically controls the growth rates of various faces of nanoparticles by selective adsorption and desorption on these surfaces [18].

CONCLUSION

Strontium-substituted lanthanum nickelate perovskite (LSNO) nanoparticles were synthesized in a nanoscale range of 53 nm by co-precipitation method using octanoic acid as a surfactant material. Morphology of nano powders seemed to be almost similar and fine spherical features. By altering the octanoic acid quantity and the calcination temperature, pH and rate of stirring, the particle size, and crystallinity of perovskite nanoparticles could be controlled. The size of the nanocrystals was measured both by XRD and SEM and the results were in very good agreement with each other.

ACKNOWLEDGMENTS

We thank University of Sistan and Baluchestan (USB) for the financial support.

REFERENCES

1. B.C.H. Steele, Materials Science and Engineering., Vol. 13, (1992), pp. 79 – 87.
2. P.J. Gellings, H.J.M. Bouw- meester (Eds.), The CRC Handbook of Solid State Electro chemistry, CRC Press., (1997), p. 630.
3. H. Arai, T. Yamada, K. Eguchi, T. Seiyama, Appl. Catal., Vol. 26, (1986), pp. 265-276.

4. A. Baiker, P. E. Marti, P. Keusch, E. Fritsch, A. Reller, J. Catal., Vol. 146, (1994), pp. 268 – 276.

5. S. Rajadurai, J. J. Carberry, B. Li, C.B. Alcock, J. Catal., Vol. 131, (1991), pp. 582 - 589.

6. L.G. Tejuca, J. L. Fierro (Eds.), Properties and Applications of Perovskite-Type Oxides, Dekker, New York., (1993).

7. M. A. Peña, J. L. G. Fierro, Chem. Rev., Vol. 101, (2001), pp. 1981- 2017.

8. P. Lukaszewicz, N. Miura, N. Yamazoe, Sensors and Actuators B Chem., Vol. 1, (1990), pp. 195–198.

9. E. L. Brosha, R. Mukundan, D.R. Brown, F. H. Garzon, J. H. Visser, M. Zanini, Z. Zhou, E.M. Logothetis, Sensors and Actuators B Chem., Vol. 69, No. 1–2, (2000), pp. 171–182.

10. C. Tofan, D. Klvana, J. Kirchnerova, Applied Catalysis., Vol. B 36, No. 4, (2002), pp. 311–323.

11. H. J. Hwang, M. Awano, J. Eur. Ceram. Soc., Vol. 21, No. 10–11, (2001), pp. 2103–2107.

12. Z. Gao and R. Wang, Appl. Catal. B: Environ., Vol. 98, (2010), pp. 147–153.

13. J. Gao, F.X. Hu and H. Yao, Appl. Surf. Sci., Vol. 252, (2006), pp. 5521–5524.

14. Q.G. Chi, W.L. Li, Y. Zhao, and W.D. Fei, J. Sol-Gel Sci. Technol., Vol. 54, (2010), pp. 286–291.

15. Z. Brankovic, K. Duris, A. Radojkovic, S. Bernik, Z. Jaglicic, M. Jagodic, K.Vojisavljevic and G. Brankovic, J. Sol-Gel Sci. Technol,Vol. 55, (2010) , pp. 311–316.

16. M. Yazdanbakhsh, H. Tavakkoli and S.M. Hosseini, S. Afr. J. Chem.,Vol. 64 , (2011), pp. 71–78.

17. H. P. Klug and L. E. Alexander, X-ray Diffraction Procedures for Polycrystalline and Amorphous Material, second ed., Wiley, New York., (1974). 18. Y. Sun and Y. Xia, Adv. Mater.,Vol. 14 ,No. 11, (2002), pp. 833-837.

Int. J. Nanosci. Nanotechnol., Vol. 10, No. 1, Mar. 2014, pp. 51-60

Influence of Adding SiC on Microstructure and Electrical Properties of ZnO-based Nanocomposite Varistor

M. Azadmand[*1], A. Nemati[2], K. Arzani[1], N. Riahi Noori[3], T. Ebadzadeh[4]

1- Department of Ceramic, Science and Research Branch, Islamic Azad University, Tehran, I. R. Iran
2- Materials Science & Engineering Department, Sharif University of Technology, Tehran, I. R. Iran
3- Niroo Research Institute, Ceramic & Polymer group, Tehran, I. R. Iran
4- Ceramic department materials and energy research center, Alborz, I. R. Iran.

(*) Corresponding author: mani_azadmand@yahoo.com
(Received:15 Dec. 2013 and Accepted: 12 Jan. 2014)

Abstract:
In this research the influence of adding SiC on microstructure and electrical properties of ZnO-based Nanocomposite varistors were investigated. SiC was added with amounts of 10-0 mass% to ZnO-based varistor composition. It is found that SiC allows reaching to high threshold voltage with formation of fine-grained ZnO. Another important effect of adding SiC is formation Zn_2SiO_4 (Willemite) on the surface of SiC grains. With this effects SiC had great influence on Varistor electrical properties. On the other hand relative density decreased with increasing percentage of SiC in the composition. Hence with adding SiC to the composition, the threshold voltage of varistors (VT) and non-linear coefficient (α) increased at first and then decreased with increaseing of porosity. Also Current leakage decreased at first and then increased with adding more SiC. Also ZnO powder size effect on the final properties was examined in this reasearch by using submicron size and Nano size ZnO powder. The best achieved electrical result was threshold voltage as large as 4220 V/cm and non-linear coefficient α=44 that were gained by using of Nano ZnO powder and adding %4 SiC to the composition.
Keywords: *Electrical properties, Grain growth, Nanocomposite, SiC, Varistor, ZnO.*

1. INTRODUCTION

Varistors (variable resistors) are voltage-dependent resistors with a symmetrical V/I characteristic curve whose resistance decreases with the increase of voltage. The voltage dependence of varistors or VDRs (voltage dependent resistors) may be approximately characterized by the formula

$$I = KV^{\alpha} \quad (1)$$

Where K is constant and α denotes the non-linearity exponent and in this way may be interpreted as a measure of the steepness of the V/I characteristic [1-2].

The first known ceramic material showing that property is the silicon carbide (SiC). This ceramic material consists of SiC particles (ranging from 50 to 100 μm in size), intimately bonded to a silica rich vitreous matrix.

Single phase BeO doped SiC varistors was developed by hot isostatic pressing. Despite having superior electrical resistance than multiphase SiC varistors, the ceramic's non-linear coefficient remained low (α=5).

On the other hand high non-linear varistor materials (α=50) were developed by Matsuoka. Those ceramics have complex chemical composition constituted by ZnO as major component, and small amounts of Bi_2O_3, Sb_2O_3, CoO, MnO_2 and Cr_2O_3. Their microstructure is multiphase being formed by ZnO grains as predominant phase and many

Table 1: *Chemical composition of samples*

Composition	mass %					
	ZnO	**SiC**	**Bi_2O_3**	**Sb_2O_3**	**CoO**	**PVA**
A	95	0	3	1.5	0.5	0.75
B	93	2	3	1.5	0.5	0.75
C	91	4	3	1.5	0.5	0.75
D	89	6	3	1.5	0.5	0.75
E	87	8	3	1.5	0.5	0.75
F	85	10	3	1.5	0.5	0.75

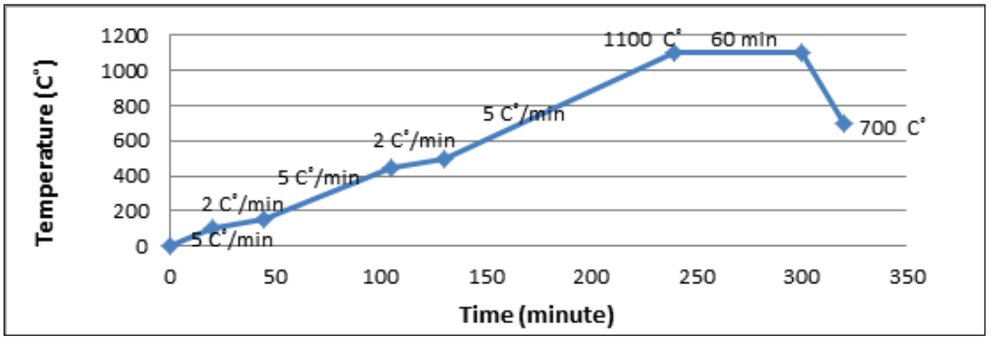

Figure 1: *Rate of heating varistor samples*

other phases like the spinel ($Zn_7Sb_2O_{12}$), pyrochlore ($Zn_2Bi_3Sb_3O_{14}$) and several polymorphic phases of bismuth oxide, distributed in the structure [3].

ZnO based varistors exhibit highly non-linear current–voltage characteristics which find application in the field of protection gainst transient voltage surges. In doped ZnO ceramics non-linearity coefficients as high as α=70 can be achieved. In standby, the varistor is subjected to a voltage below its characteristic breakdown voltage and only a leakage current pass through the bulk specimen. During transient surge the voltage between electrodes exceeds the breakdown voltage and the varistor becomes highly conductive diverting the current to ground and so protecting the circuit.

The non-linear response originates on its polycrystalline microstructure and more specifically on detailed processes occurring at the grain/grain interfaces. By proper doping, the near grain boundary region becomes highly resistive while the grain interior turns into conductive, and electrostatic potential barriers build up at the grain boundaries due to charges being trapped at interface states [4].

In fact in Ceramic varistors based on the ZnO–Bi_2O_3–Sb_2O_3 system the characteristic non-linear current-voltage response is a consequence of their microstructure and electronic structure. Non-ohmic behavior is due to the presence of electrically active grain boundaries, formed by an intergranular Bi_2O_3-rich phase that separates the semiconducting ZnO grains. Besides Bi_2O_3, other oxides enter in minor proportions into the varistor composition (Sb_2O_3, CoO, MnO_2 and Cr_2O_3). Their role is to improve the electrical response [5].

With consideration that ZnO based varistors and SiC based varistors are used as two important generation of varistors, it seems that there is a vacant place in research papers to examine the properties of ZnO-SiC composite as a varistor. We know that SiC has a very strong covalent bond. As a tough material SiC can prevent the ZnO grain growth and help to have tinier microstructure. In the present work, influence of amount of added SiC and also affection of using Nano size ZnO powder on microstructure, final density, and current–voltage (I–V) characteristics of ZnO-based varistor ceramics has been investigated.

2. EXPERIMENTAL

The basic formulation and preparing process in current research were chosen like conventional varistor formula and process. Analytical grades of ZnO (Zinchem, 300-900 nm), ZnO (Nano Amor, 20 nm), SiC-β (Nano Amor, 45-55 nm), Bi_2O_3 (Nano Amor, 90-210 nm), Sb_2O_3 (Nano Amor, 90-210 nm), CoO (Nano Amor, 90-210 nm), and PVA (Sigma), were used in this work. SiC-β was chosen because mobility of SiC-β is higher than SiC-α and thus the electrical resistance of SiC-β is lower than SiC-α [6]. In this paper the samples which made by Nano size ZnO powder are called Nano samples and the samples which made by Submicron size ZnO powder are called Submicron samples. The composition of the samples are shown in Table 1.

2.1. Sample preparation

The samples were prepared by conventional method. Table 1 shows the chemical compositions of samples prepared in this research. The oxide powders were weighed and then mixed during 20 min with Alumina balls and distilled water in fast mill. The Aqueous slurry obtained was dried in 80°C during 24 h. Then dry milling of the dried batches was carried out during 20 min in fast mill without water just by alumina balls. The batches were molded in discs of 20 mm diameter and 3 mm in thickness under pressure of 100 Mpa by using hydraulic isostatic press. Then the green bodies were sintered at 1100°C for 1 h. The maximum sintering temperature was chosen based on other researcher experiences [7-8].

The rate of heating is shown in Figure 1. It was chosen with considering some physical and chemical reactions during the heating. Some of the important chemical reactions are as below [1, 9-10].

$$Sb_2O_3\ (s) + O_2\ (527°C) \rightarrow Sb_2O_5\ (l) \quad (2)$$

$$Sb_2O_5\ (l) + ZnO\ (s)(700\text{-}800°C) \rightarrow ZnSb_2O_6\ (s) \quad (3)$$

$$ZnSb_2O_6\ (s) + 6ZnO\ (s)(>800°C) \rightarrow Zn_7Sb_2O_{12}\ (s) \quad (4)$$

$$2Zn_2Bi_3Sb_3O_{14} + 17ZnO\ (950\text{-}1050°C) \rightarrow 3Zn_7Sb_2O_{12} + 3Bi_2O_3 \quad (5)$$

$$3ZnSb_2O_6\ (s) + 3Bi_2O_3\ (s) + ZnO\ (s)(900\text{-}700°C) \rightarrow Zn_2Bi_3Sb_3O_{14}\ (s) \quad (6)$$

2.2. Density measurment and Analyzing of microstructure and phases

The density of the pellets was measured by Archimedes method.

$$\rho = W_d / W_w - W_s \quad (7)$$

$$\%RD = (\rho / \rho_{th}) \times 100 \quad (8)$$

Where ρ is density, Wd is dry weight, Ww is wet weight, Ws is soaking weight, ρth is theoretical density that were measured for each composition, and %RD is relative density. To observe the microstructure scanning electron microscope (SEM, TESCAN-VEGII XMU, Czech) was utilized. In order to remove ZnO from surface and emerge grain boundaries, the pellets were polished and etched with 5 molar NaOH solution. Also the samples were coated with gold to be ready for SEM analyzing. The crystalline phases were identified by an X-ray diffractometer (STADI-MP, Germany) using 40 KV voltage and 30 mA amperage and Cu Kα as a radiation source.

2.3. Measurement of V–I characteristics

For electrical varistor test, the pellets were polished and coated by conductive Carbon onto both faces with using conductive Carbon spray (KONTAKT CHEMIE, Belgium). For avoiding of surface current effect, the bodies were coated on the side part by an insulator epoxy resin. The I–V characteristics were measured at low currents until 10 mA under continuous voltage. The voltage–current (V–I) characteristics were measured by using a V–I source/measure unit. The nominal varistor voltages (V_N) (breakdown voltage is the voltage at which the varistor switches from a highly resistive to a highly conductive state) at 1 and 10 mA and the threshold voltage V_T (V/mm) (breakdown voltage/

unit thickness of varistor ceramic) were measured. $V_T=V_N$ (1mA)/d, where d is the thickness of the sample in mm) and the non-linear coefficient α (α=log(I_{10mA}/I_{1mA})/log(V_{10mA}/V_{1mA}) =1/log (V_{10mA}/V_{1mA}) according to the equation describing the V–I non-linearity of the varistor ceramics $I=KV^{\alpha}$) were determined. The leakage current (I_L) (the current through the varistor in the pre-breakdown region of the V–I characteristic) was measured at 0.75 V_N (1mA) [7].

3. RESULTS AND DISCUSSION

Six different varistor samples with different compositions were constructed. Figure 2 shows SEM micrographs of ceramic varistors sintered 1 h in 1100˚C with 0, 2, and 6 mass% of SiC content. As can be seen, basically, the growth of ZnO grains was prevented by SiC grains and therefore the average of ZnO grain sizes decreased as the amount of SiC increased. From the other point of view, densification has been limited by increasing the amount of SiC. With the increase of mass% of SiC from 0% up to 10 % in the composition, the average of ZnO grain size decreased from 4 μm to 2 μm and the amount of porosity increased from 6% up to 25%.

So it will have two different effects on the varistor properties: 1-decreasing ZnO grain size 2-increasing the amount of porosity. For investigation of ZnO initial powder size effects on the final microstructure of varistors, series of samples were prepared with using ZnO nano size powder with the same formula. As can be seen in Figure 2 the average of ZnO grains in the samples content nano ZnO didn't have sensible difference to the samples which prepared by submicron size ZnO.

The increasing of porosity with adding SiC was verified by measuring density. The density of samples was measured by Archimedes method. The results are shown in Figure 3. It can be realized a sensible decrease in density of samples from 94% to 73% with the increasing amount of SiC from 0% to 10% in the composition. This event might be occurred by two reasons. Firstly SiC seeds as a physical barrier can prevent the ZnO grains to reach each other during the sintering. Hence SiC prevents densification process. Secondly vaporization of Carbon due to oxidation of SiC in high temperature can make porosities in the microstructure of samples. A similar rate of decreasing in density was occurred in nano samples. But nano samples revealed a higher density in comparison to submicron samples. In nano samples the average of relative density was about 2% higher than Submicron samples.

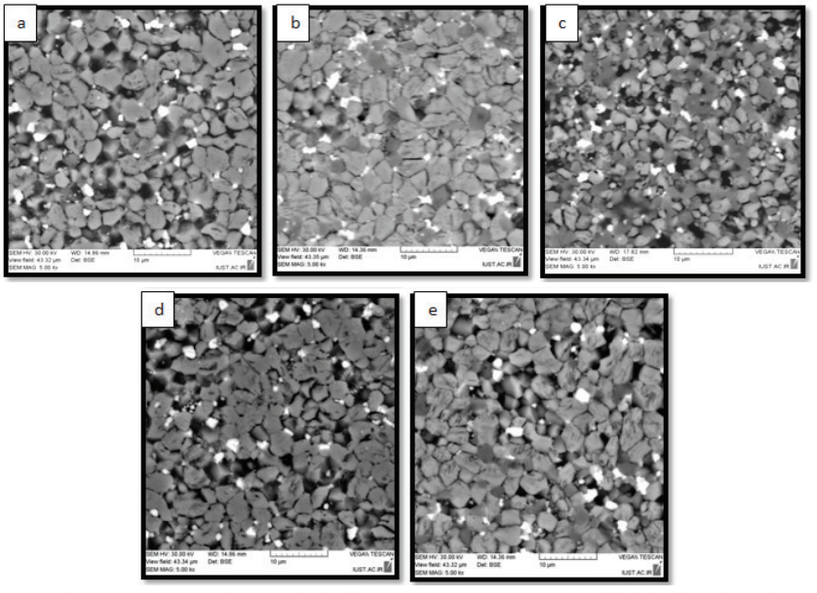

Figure 2: *SEM image of varistor samples with different composition: (a) 0% SiC with submicron ZnO; (b) 2% SiC with submicron ZnO; (c) 6% SiC with submicron ZnO; (d) 0% SiC with nano size ZnO; (e) 2% SiC with nano ZnO*